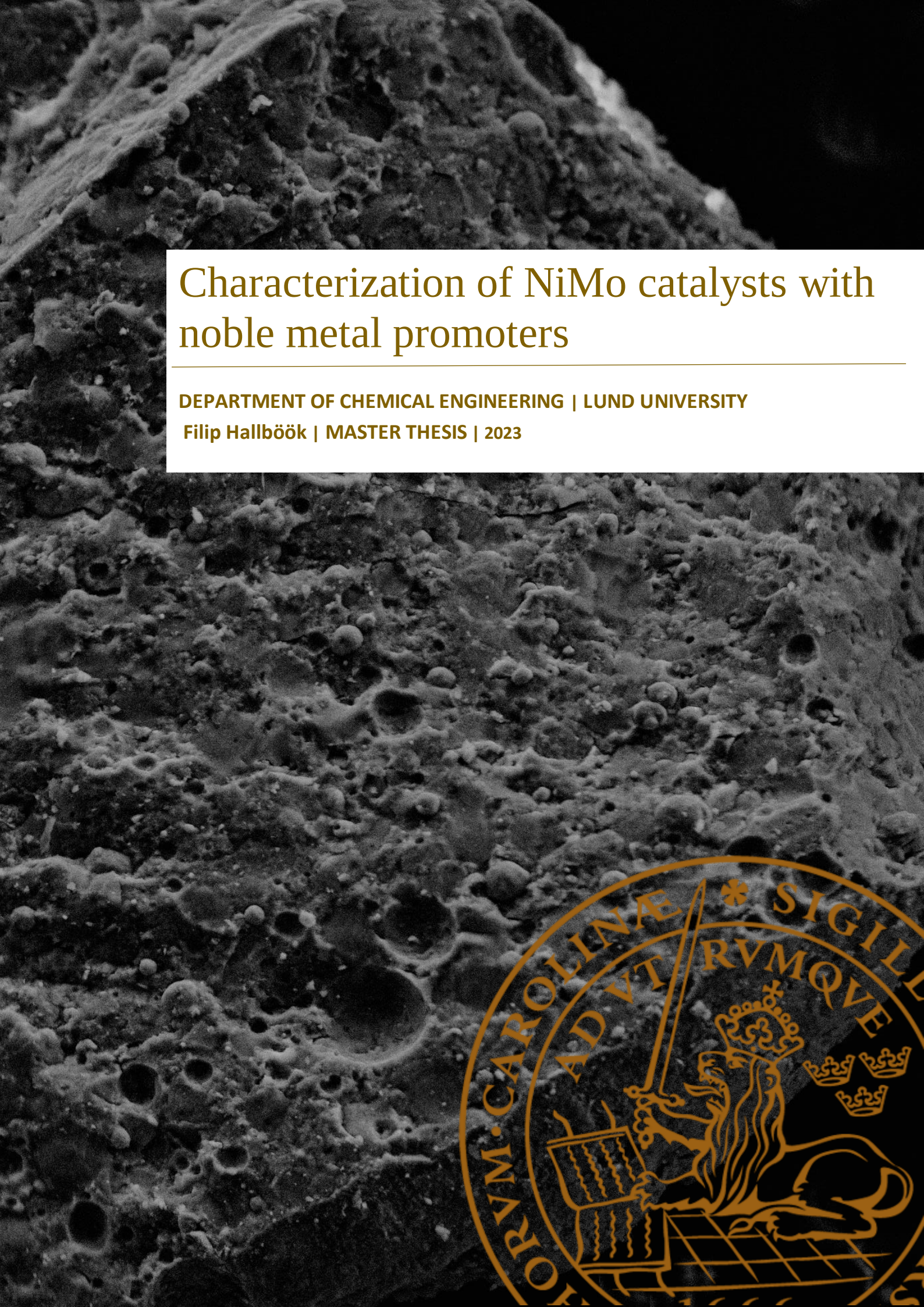

Characterization of NiMo catalysts with noble metal promoters

DEPARTMENT OF CHEMICAL ENGINEERING | LUND UNIVERSITY

Filip Hallböök | MASTER THESIS | 2023

Characterization of NiMo catalysts with noble metal promoters

by

Filip Hallböök

Department of Chemical Engineering
Lund University

February 2023

Supervisor: **Associate Senior Lecturer Sara Blomberg, PhD**
Examiner: **Hanna Karlsson PhD**

Picture on front page: SEM micrograph of a Pt-NiMo catalyst granulate

Postal address
P.O. Box 124
SE-221 00 Lund, Sweden

Visiting address
Getingevägen 60

Telephone
+46 46-222 82 85
+46 46-222 00 00
Telefax
+46 46-222 45 26

Acknowledgements

I wish to thank my supervisor Sara Blomberg for providing support and help throughout my work with this project. I would also like to extend a big thank you to Tove Kristiansen for synthesizing the catalysts characterized in this project and for many interesting and valuable discussions.

Furthermore, many thanks to all my colleagues at the Department of Chemical Engineering for the very inclusive and warm atmosphere and all the conversations and company around the fika and lunch table.

Populärvetenskaplig sammanfattning

Klimatförändringar är en av vår tids stora utmaningar. För att kunna möta dessa finns det ett brådskande behov av att minska vårt stora beroende av fossila bränslen. En lovande råvara för produktion av förnyelsebara och koldioxidneutrala bränslen är bioolja. Bioolja kan användas som ett substitut för råolja i raffinaderier och produceras från biomassa, vilket innebär att den kan agera som ett förnyelsebart substitut. Bioolja kan produceras med en process som kallas för pyrolys där exempelvis träflis eller annan biomassa snabbt hättas upp och förångas. De resulterande ångorna kyls sedan ner och har då en sammansättning som kan liknas med råolja, vilket främst innehåller kol- och väteföreningar som är grunden för de bränslen som används idag. Bioolja producerad från biomassa har dock en betydande skillnad, en hög halt av kemiska föreningar med syre. Detta är en konsekvens av den kemiska sammansättningen av biomassan biooljan producerats från och detta påverkar bränsle-egenskaperna hos oljan negativt. På grund av detta behöver biooljan uppgraderas innan den kan användas. Ett av det viktigaste stegen kallas för katalytisk hydrodeoxygenering (HDO) där syreatomerna i oljan selektivt tas bort.

Som namnet antyder är detta en katalytisk process vilket innebär att en så kallad katalysator krävs för att processen ska fungera. Katalysatorer består ofta av metaller som hjälper reaktionen att fortgå ofta vid en lägre temperatur och med mindre biprodukter. Den katalysator som mest framgångsrikt har använts i HDO-processen är baserad på nickel och molybdensulfid, där molybden är den aktiva komponenten som underlättar reaktionen, medan nickel agerar som en så kallad promoter, det vill säga ett ämne som underlättar reaktionen utan att vara direkt involverad. Ett viktigt steg i att göra denna process mer effektiv och ekonomiskt gångbar är vidareutveckling av dessa katalysatorer.

I denna studie undersöktes effekterna av att tillsätta små mängder av ett tredje ämne, en ädelmetall, till dessa katalysatorer. Mer specifikt undersöktes ädelmetallerna platina, palladium och iridium. Tanken med tillsatsen av små mängder av dessa metaller är att undersöka om det finns synergistiska effekter tillsammans med nickel och molybden. För att se om dessa finns undersöktes metallernas reduktionsegenskaper. Detta gjordes genom en metod som kallas för Temperatur-Programmerad Reduktion (TPR), där katalysatorerna utsätts för ett flöde av vätgas medan temperaturen ökar. Genom att studera hur reduktionen av katalysatorn förändras när man tillsätter ädelmetallerna kan slutsatser dras kring dessa synergistiska effekter. Två tillverkningsmetoder av katalysatorerna undersöktes också, där tillsatsordningen av ädelmetallen ändrades för att undersöka om detta påverkar hur katalysatorn beläggs med ädelmetallen. Alla tre ädelmetaller hade en stor inverkan på reduktionen av molybden och nickel. De studerade ädelmetaller uppvisade alla en synergistisk effekt, men effekten av att tillsätta iridium skiljde sig från platina och palladium. För iridium kunde en övergång till metalliskt iridium observeras innan nickel och molybden reducerades medan för platina och palladium skedde detta samtidigt. Detta tyder på att den synergistiska mekanismen är annorlunda för iridium. Sammanfattningsvis visar denna studie på att tillsatsen av de undersökta ädelmetallerna ledde till enklare reduktion av den resterande katalystorn.

Abstact

To be able to face the challenges brought on by climate change there is an urgent need to reduce the heavy dependence on fossil fuels. Bio-oil is one such renewable and carbon-neutral replacement that has shown promising potential. A key step in making bio-oil commercially feasible is improvements of the upgrading processes of the bio-oil. One such upgrading process is catalytic hydrodeoxygenation (HDO), which has been developed using mainly molybdenum sulfide (MoS_2) catalysts. One method to further develop the process is to improve the catalyst performance by the addition of promoters. Nickel and cobalt has commonly been used as promoters for MoS_2 catalysts, but there is potential for further improvement of the catalysts by addition of noble metals as promoters.
In this study the promoting effects of adding the noble metals iridium, palladium and platinum using two different impregnation methods were investigated. This was done by studying the reduction characteristic of the new catalysts using Temperature Programmed Reduction (TPR), together with chemical characterization using Scanning Electron Microscopy - Energy Dispersive Spectroscopy (SEM-EDX). All the studied noble metals induced a significant change of the reduction characteristics of the catalysts, by lowering the reduction temperature of the Ni-Mo oxide. Two different promoting mechanisms could be identified. The addition of iridium resulted in a separate reduction of IrO_2 with a subsequent promoting of Ni-Mo oxide, while the addition of platinum and palladium gave rise to simultaneous reduction of the noble metal and the surrounding Ni-Mo oxide. One possible mechanism for the promoting by iridium is hydrogen spillover. The differing behaviours of palladium and platinum could indicate a different behavior, for example the ability to be dissolved in the Ni-Mo oxide structure, creating nucleation sites for the reduction process. The formulation method used was found to have the largest effect on the iridium catalysts, where co-impregnation improved the promoting abilities. No significant changes were found for palladium and platinum. Overall this study has found promising results in the use of noble metals as promoter for Ni-Mo catalysts, and further studies are warranted.

Contents

1 Introduction

The need to reduce the heavy reliance on fossil fuels in modern society is clear, both from the perspective of its finite quantity, and more urgently, its high impact on global warming. To combat this growing problem there is an urgent need to develop renewable and carbon neutral fuels to be used in areas such as in the transport sector. Current day renewable combustion fuels include fuels such as bio-diesel and bio-ethanol. These fuel types are commercially available and to some extent already integrated into the fuel economy. However, a large majority of the renewable fuels used today are so-called first-generation bio fuels. First generation biofuels refer to what types of feedstocks that are used in the production of the fuels. Both bio-diesel and bio-ethanol very often uses feedstocks which stand in direct competition with agricultural land, used for the production of food and other essential products needed for direct human consumption.[1]

One promising pathway to broaden the types of biomass which can be used for fuel production is the production of bio-oil using a pyrolysis process. The benefits of producing bio-fuels using such a process is that it is possible to utilize a more diverse biomass feedstock such as waste streams originating from wood or agricultural waste. Fuels produced from these types of more abundant and less constricted feedstocks are called second generation bio-fuel and the development of these processes is of great importance for the feasibility of a complete switch to renewable fuels. In the pyrolysis process a non-specific biomass is flash heated to a high temperature of over 800 °C, in which the cellulose and other organic compounds are cracked into smaller molecules. The outflow from the pyrolysis reactor is then separated into condensable and non-condensable products, of which the condensable product is called bio-oil. Bio-oil produced using this method inherits the high oxygen content of the biomass which causes problems during storage and further processing of the oil. The exact composition of the oil will depend on the feedstock used, however an elemental composition of 30-50% oxygen is common. [2] The high oxygen content increases the water solubility of oil allowing for water to stay dissolved, which directly reduces the heating value. The oxygen containing species of the oil also increases the reactivity which can cause the oil to polymerize if kept at elevated temperatures. The pH of bio-oil is generally low due to acids present which can cause problems in processing due to corrosion. Due to all these factors, upgrading of bio-oil is key to make it suitable for fuel applications. Another important factor is to be able to integrate bio-oil into existing refinery pathways, which would reduce the initial capital costs for bio-oil processing. [1]

One of the most promising processes for the upgrading of bio-oil is a catalytic process known as hydrodeoxygenation (HDO). [3] This process has many similarities with the common refinery process Hydrodesulfurization (HDS) and the development of the HDO process has in a large part been based on knowledge from the HDS process. [4] The overall reaction of the HDO process involves the reaction of hydrogen with the oxygen containing species of the bio-oil and the large amount of different oxygen containing species present in bio-oil makes the reaction very complex. [5] Several types of catalysts are used in the HDO process but the most common are supported transition metal oxides and sulfided metals. [3, 5] This study is focused on the development of one type of such metal catalyst, nickel-molybdenum oxide supported on alumina. This catalyst was originally developed for the use as a catalyst in the HDS process but has shown great potential in the HDO process as well. [6, 4] There have been several studies documenting a promoting effect of adding small amounts of noble metals to sulfide and phosphides catalysts for HDO and similar processes such as hydrodenitrogenation (HDN) and HDS. [7, 8] With these documented effects on similar catalysts, this study aims to characterize any promoting effect of adding noble metals to nickel-molybdenum oxide catalysts.

1.1 Aim

The aim of this study was to evaluate the promoting effect of the addition of the noble metals platinum, palladium and iridium to the formulation of Nickel-Molybdenum based HDO catalysts. The order of impregnation in the syntesis of the catalyst was investigated. More specifically if there is any effect of impregnating the noble metals simultaneously as the nickel compared to afterwards. The promoting effect was evaluated on the oxide form of the catalysts, through the determination of their reduction characteristics using Temperature Programmed Reduction (TPR). In order to perform quantitative analysis using this method, this project also includes the development of a quantitative analysis method and calibration of the TPR instrument. Further characterization of the catalysts to verify the chemical composition was do done using Scanning Electron Microscopy (SEM) together with Energy dispersive X-ray Spectroscopy (EDX).

2 Theory

2.1 Heterogeneous Catalysts

Heterogeneous catalysts play a major role in modern large-scale chemical industry. [3] Most heterogeneous catalysts consist of two component types, carrier and active phase. The carrier plays the role of dispersing the active phase onto a large surface area while itself being chemically and thermally stable to retain the active materials throughout operation. Common carriers are typically made out of alumina or silica, due to their chemical stability and ability to form a porous, high surface area matrix on which the active metals can be bound. The active phase of the catalysts is then deposited onto the support, the active phase can be made out of one or more components, commonly metals. If there are more than one active component used they are commonly deposited in a sequential order. It is of great importance to have a good metal dispersion and a small crystallite size in order to achieve a high activity.

One method which is commonly used in industry and can achieve these criteria is incipient wetness impregnation (IWI). In this method dissolved metal salts are used as the source of the active metal. To determine the concentration of the metal salt solution, the amount of water that the catalyst support can absorb needs to be measured. This is done by adding water drop wise until the support is visually saturated, the amount of water required is then measured via the weight change of the support. Once the water saturation level of the support is known the desired loading of the active metal can be dissolved in the equivalent amount of water/solvent. [9] The impregnated catalyst is then dried and calcinated to drive of water and volatile compounds, leaving the active metal finely dispersed on the support. To promote the formation of small crystallites, chelating agents such as citric acid can be added to the metal salt solution. This prevents nucleation of metal crystallites before the calcination and can lead to a more finely dispersed active phase. [9]

2.2 NiMo catalysts

Molybdenum-sulfide catalysts have commonly been used in different hydrotreatment processes where removal of heteroatoms such as nitrogen and sulfur are wanted. One of the most studied applications of the MoS_2 based catalysts is the HDS process, which is a critical step in oil refining. Sulfur levels in modern combustion fuels are heavily regulated due to their large environmental impact and within the refining process sulfur can, even at low concentrations, poison the noble metal catalysts used in catalytic cracking further downstream in the process.[10] Even though the catalytic activity is provided by the Mo oxide or sulfide a second metal, most commonly nickel or cobalt, is often added with the purpose of acting as a promoter. Promoters can be described as compounds that indirectly increase the activity, by for example changing the crystal structure of the catalytically active material. For MoS_2 catalysts a mechanism for the promoting effect of nickel and cobalt was proposed by Lauritsen et al. In this widely accepted theory the addition of cobolt was found to cause a change in the morphology of the MoS_2 crystallites. This is thought to effect surface structure inducing vacancies in the structure on which the oxygen containing species may adsorb. [11, 3] The oxide version of the NiMo catalysts have also shown a catalytic activity in the HDO processes, though not to the same extent as the sulfide. [5] However, the oxidized NiMo catalyst is also used as a precursor for the sulfidation, and the sulfidation is often done *in-situ*, meaning in the HDO reactor before or during the HDO reaction itself. The structure of the oxide precursor has also been found to be of great importance for the performance of the sulfide catalyst. [12] The oxide structure formed by the Ni-Mo system is Ni(II)Mo(IV)O_4, which has three well defined main polymorphs α-$NiMoO_4$, β-$NiMoO_4$ and its hydrated form nH_20 •$NiMoO_4$. [12]

The reduction behavior of the Ni-Mo oxides has been shown to be a predictor of catalytic activity for sulfided NiMo catalysts in both HDO and HDS reactions. [13, 14] Brito et al. studied the sulfidation and HDS activity of the α-, β- and hydrated polymorphs of $NiMoO_4$ and found a direct correlation between both a higher degree of sulfidation and a higher HDS activity with a lower reduction temperature. [13]

Noble metals themselves have been studied as potential catalysts for both HDO and HDS, and have been found to have high activity both in their metal and sulfide form. [15, 16, 17] However, due to their very high price several studies has also looked into using noble metals not as the primary catalytic element but as low concentration promoters of a cheaper active material. [18, 19, 7] Several authors

has also reported enhanced reduction characteristics by addition of noble metals, which as mentioned previously has been correlated with improved catalytic activity for NiMo catalysts as well. [7, 19]

2.3 Temperature Programmed Reduction

Temperature programmed reduction is a characterization method for solid materials where the reduction characteristics of a material is probed. This is done by passing a reducing gas, such as hydrogen, over the sample while varying the temperature. To monitor the reduction reaction the gas composition before and after interaction with the sample is measured and the change in reducing gas concentration can therefore be correlated with a reduction event. [20, 21] When using hydrogen as the reducing gas the reduction of a metal oxide MO_x is described in Reaction 1 below.

$$\mathrm{MO}_x + \mathrm{XH}_2 \longrightarrow \mathrm{XH}_2\,\mathrm{O} + \mathrm{M} \qquad \{1\}$$

To measure the composition of the outflow gas the most common detectors are thermal conductivity detectors (TCD) and mass spectrometers (MS). A TCD measures the conductivity of the gas that passes through the detector, and has the advantage of having a very high sampling rate and high sensitivity. However, due to the fact that this detector type only measures the total thermal conductivity of a gas, if there are more than two gases present in a gas blend, determining the concentration of each gas in that mixture is not possible. This will mainly be relevant when analyzing reactions where several types of products can be formed, such as analysis of coking with Temperature Programmed Oxidation (TPO) or Temperature programmed Reaction (TPRx). Another consequence of measuring gas concentration via its thermal conductivity is that the sensitivity of the measurement is dependent on the difference in thermal conductivity between two gases in a mixture. This will dictate what carrier gas is chosen for the wanted analysis gas to make sure that the difference is as large as possible. With a MS the composition of the gas can be measured directly and more importantly, the composition of gas blends with more than two components can also be measured directly.

The reduction reaction which is measured in a TPR experiment is a rather simple reaction in principle but in practice the properties of the sample such as particle size, support interaction and particle morphologies can have a large effect on the kinetics of the reduction. In addition, TPR is very sensitive to experimental parameters such as heating rate, gas flow rate and the amount of sample analyzed. [22] Making a direct comparison of TPR results with literature is therefore challenging. Furthermore, the large impact of experimental parameters creates the need for method development for each type of sample, and it is very important to keep the analysis conditions constant when comparing results.

Quantitative TPR is based on the same principles as qualitative TPR, however by running a series of calibration experiments, the TPR reduction profile can be calibrated to allow for the readout of the consumed amount of reducing gas, most commonly hydrogen.

2.4 Reduction behavior of Nickel and Molybdenum oxides

To be able to interpret the reduction behavior based on TPR results, it is necessary to have a understanding of which oxides the metals in the studied system can form. Pure molybdenum is known to form two types of oxides when oxidized, $Mo(VI)O_3$ and $Mo(IV)O_2$, where the trioxide is expected as the main product of a high temperature oxidation. [23] When oxidized, nickel is known to form Ni(II)O primarily, other oxide forms exists but they have not been found to be stable at higher temperatures. Introducing aluminum, through for example supporting the nickel on alumina, allows for the formation of $NiAl_2O_4$, which has been found to complicate the reduction profile of supported nickel oxides.[24]

One factor that makes distinguishing a mixture of the two mono-metallic oxides, MoO_3 and NiO, difficult from the bimetallic $NiMoO_4$, which is sought after for HDO catalysts, is that the total oxidation state is the same at +8. This will make using quantitative TPR as a method for detecting the formation of this compound difficult, but a change in reduction temperature can be expected by the different structure, and this has been shown in literature[12].

The reduction characteristics of $NiMoO_4$ was studied in the form of bimetallic Ni-Mo nanoparticles by Nordlander [25]. The author found that the $NiMoO_4$ nanoparticles were reduced after being subjected to a temperature of 710°C and had been segregated into separate nickel and molybdenum phases. The

nickel was found to be fully reduced to metallic nickel, but the oxidation state of the molybdenum could not be determined.

The possible oxides formed by the noble metals are also important for the interpretation of the TPR results. Iridium is known to form Ir(IV)O_2, as its most commonly occurring oxide. Other occurring oxides exist such as Ir_2O_3, however this oxide is not known to be stable at an elevated temperature in a oxidative environment. [26] Platinum has been found to form two main oxides, Pt(II)O and Pt(IV)O_2 , while the only commonly occurring palladium oxide is Pd(II)O. [27, 28] In theory it is possible that the addition of the noble metals could form tri-metallic oxides such as nickel-molybdenum-iridium oxides, however to the authors knowledge no such structures have been characterized.

2.5 Principles of Scanning Electron Microscopy (SEM)

Scanning electron microscopy (SEM) is a commonly used method for both morphological and chemical characterization of solid materials. The working principle of SEM is fundamentally different than optical microscopes where light passes through the sample and is reformed into an image using optical methods such as lenses or mirrors. In SEM the image is formed by scanning an electron beam, that has been focused into a spot over the sample, and detecting secondary or back scattered electrons emitted from the sample. When the electrons collide with the sample several events can occur, the high energy incoming electron can inelastically interact with an atom in the sample which results in the emission of x-rays and low energy secondary electrons. These secondary electrons are what is most commonly measured when imaging the morphology of a sample.

2.5.1 Principles of Energy Dispersive X-ray Spectroscopy (EDX)

The X-rays generated by the inelastic interactions between the electrons and the sample can provide chemical information about the sample. The inelastic interaction between the incident electrons and the sample causes inner shell electrons to be exited into a higher energy state. When these high energy electrons relax into their more stable inner shell configuration the energy difference between these two energy states is released as an X-ray photon. This will result in X-ray photons having an energy which can be related to a specific electron transition within the atoms of the sample. By measuring the X-rays emitted from a sample being bombarded with electrons an X-ray spectra can be collected. By identifying the X-ray lines present in the spectra the composition of the sample can be determined. [29] To quantify the elements detected in the sample the Cliff-Lorimer method is commonly used. In this method the relative intensity of the X-ray lines together with a sensitivity factor is used to calculate the relative atomic/weight percentage. The Cliff-Lorimer equation is shown below:

$$\frac{I_A}{I_B} = k_{AB}\frac{n_A}{n_B}$$

Where I_A and I_B represent the intensities of X-ray lines for two different elements, A and B. n_A and n_B represent the atomic fraction of these same two elements. The sensitivity factor, k_{AB}, is calibrated with each instrument and these calculations are made automatically with the EDX software. Due to this effect being induced by electron crashing into the sample. EDX can be performed using the same equipment as SEM, with the addition of an x-ray detector.

One drawback of doing imaging at the same time as chemical characterization is that the optimal accelerating voltage is very different. For imaging, especially with non-conductive samples, a low acceleration voltage, around 5keV, is optimal. However, when performing EDX the energy of the incoming electrons (which is determined by the accelerating voltage) needs to be higher than the energy of the transitions of the elements in the sample, otherwise those elements cannot be detected. For example iridium has two main transitions, L_α at 9.174keV and M at 1.977keV. To be able to detect the L-Line of iridium, the accelerating voltage of the electron gun must be higher than 9.174keV and in practice a significantly higher accelerating voltage is needed to produce a good enough X-ray yield.

3 Method

3.1 Catalyst synthesis

Six different catalyst formulations were synthesized for characterization in this study. The catalysts were prepared at Hulteberg Chemistry and Engineering utilizing incipient wetness impregnation of δ-Al_2O_3. 3 pairs of nickel-molybdenum catalysts with the noble metals iridium, platinum and palladium were synthesized. In each pair two different impregnation orders were used. One sequential impregnation, where each metal was impregnated and calcinated separately, this will hereafter be known as the α-variations. The impregnation order used was: molybdenum, nickel followed by the noble metal. After each impregnation the catalyst was first dried at 120 °C for 4 hours and then calcinated at 500 °C in air for an additional 4 hours. In the second method, which can be described as a co-impregnation method. Molybdenum was impregnated in a first step, followed by drying and calcination. Then nickel was impregnated together with the noble metal in the subsequent step. These catalysts will be known as the β-variations. The same drying and calcination temperatures and times were used in the synthesis of the β-variant as in the α-variant. The wet iridium and palladium catalysts can be seen in Figure 1.

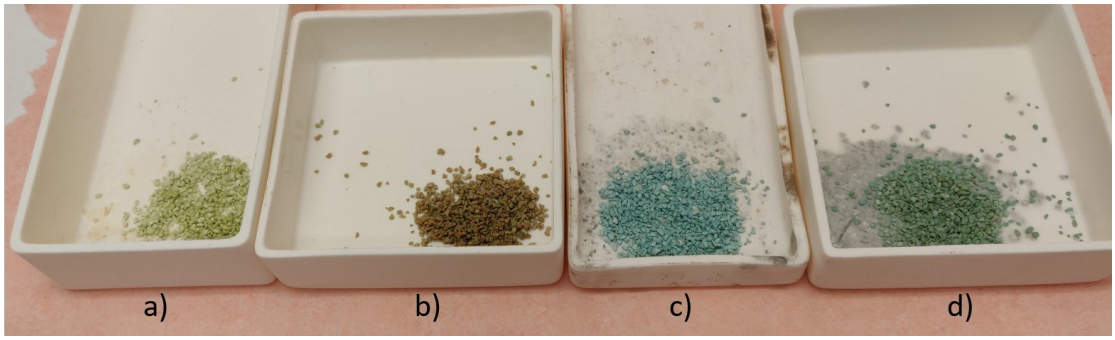

Figure 1: Wet catalysts before calcination, a) β-PdNiMo b) α-PdNiMo c) β-IrNiMo d) α-IrNiMo

As reference samples pure NiMo, nickel, and molybdenum supported on δ-Al_2O_3 catalysts were used. These catalysts were synthesised and characterized in a previous study by Blomberg et al. [30] The target composition of all catalysts analyzed is shown in Table 1.

Table 1: Target metal loadings of the analyzed catalysts. NMNiMo represents all catalysts with noble metals

Catalyst	Ni [wt%]	Mo [wt%]	Noble metal [wt%]
α-,β-NMNiMo/Al_2O_3	3.5	8.0	0.5
NiMo/Al_2O_3	3.5	8.0	0
Ni/Al_2O_3	8.4	0	0
Mo/Al_2O_3	0	14	0

An aqueous solution of Ammonium molybdate tetrahydrate was used as the molybdenum precursor. The concentration of all the aqueous metal salt solutions were prepared to correspond to the wanted metal loading seen in Table 1. Nickel was added using an aqueous solution of nickel nitrate hexahydrate. To improve the dispersion of the nickel citric acid was added to a molar ratio of 0.7 with regard to nickel. This was done to reduce the pH of the solution and to act as a chelating agent. The noble metals were prepared as aqueous solutions as well, with the precursor salt used being; iridium acetate, palladium nitrate and platinum nitrate.

3.2 Characterization

3.2.1 Temperature programmed reduction

Temperature programmed reduction was performed using a 3Flex (Micromertics, USA) equipped with a TCD detector. Catalyst samples of approximately 0.26g were analyzed this amount was chosen to achieve an active oxide amount of 35mg. The samples were placed in a quartz reactor surrounded by quartz wool and lowered into a furnace which was heated from 35 to 1100°C with a heating rate of 10 °C/min. During the entire temperature ramp the sample was subjected to the analysis gas consisting of 10% H_2 in Ar (flowrate of $50cm^3$/min). To condense the formed water the gas flow was passed through a cold trap with an Isopropanol/Liquid nitrogen slurry cooling the analysis gas to approx. -80°C.

For the quantitative analysis of the TPR results, a series of calibration measurements were done. An illustration of the setup of the calibration of the quantitative TPR can be seen in Figure 2.

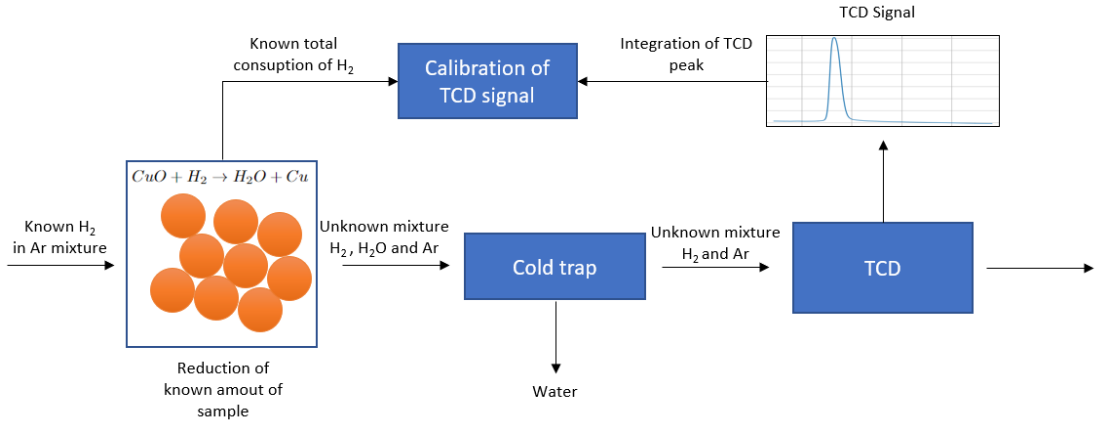

Figure 2: Illustration of the procedure for calibration of the quantitative TPR

The TCD signal is directly proportional to the total thermal conductivity, which in turn is proportional to the composition of the gas stream passing though the detector. As a calibration standard CuO powder was used with sample amounts ranging from 15mg to 50 mg. The same analysis gas, flowrate and temperature ramp was used, with the only change in experimental conditions being the temperature endpoint which was set to 600°C, as the reduction of CuO happens at 400°C. By analyzing these pure calibration samples it is possible to know how much hydrogen has been consumed after full reduction of the sample. By integrating the TCD signal, the area of the reduction peak can be calculated. This area will be directly proportional to the amount of consumed hydrogen and by performing a series of experiments with a varying sample amount, a calibration curve can be constructed.

3.2.2 SEM-EDX

Chemical characterization and high-resolution imaging were performed using an SEM (JSM-6700F, JEOL Japan) equipped with cold field emission gun operated at 20 keV and a large-area SDD for EDX. The two iridium catalysts were analyzed without any improvement of conductivity of the surface however due to the significant charging when analyzing those two sample the following two platinum catalysts were analyzed with a 20nm thick carbon layer that was deposited before analysis. The EDX-quantification was performed using the AZtec II (Oxford Instruments) software utilizing the Cliff-Lorimer method.

4 Results

4.1 Catalyst composition and morphology

The compositional analysis was done by area-based spectrum collection. X-rays are collected by scanning the selected area of the sample with the electron beam and collecting all the detected x-rays into a combined spectrum. These collection areas are marked in Figure 3 and 4 by S1-4. Due to the poor conductivity of Al_2O_3, significant charging occurred on the samples, which can be seen by the white areas in both a) and b) in Figure 3. This made high resolution imaging challenging, as charging of the surface of the particles distorts the incoming electrons.

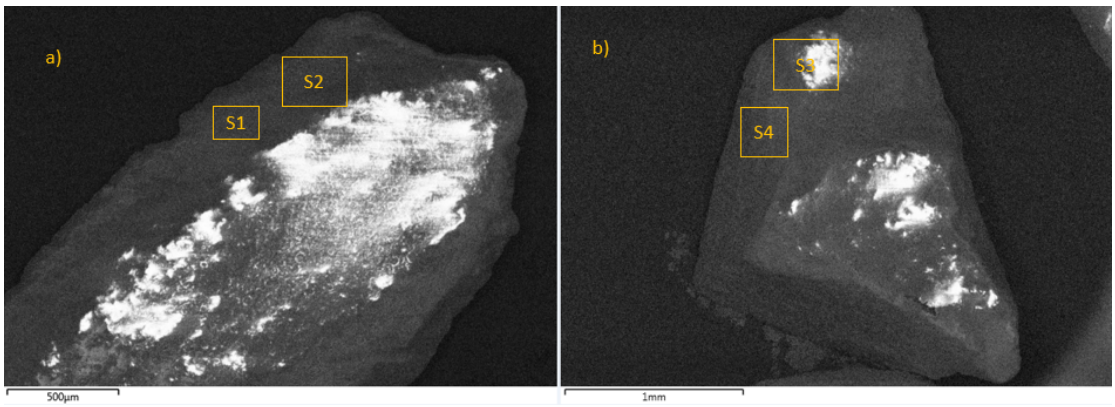

Figure 3: SEM micrographs with EDX collection areas highlighted, S1-S4 a) α-IrNiMo catalyst particle with EDX b) β-IrNiMo catalyst particle

This charging does not affect the composition analysis done via EDX and the results of the quantification of the X-ray spectra captured of the two formulation of the IrNiMo catalysts are shown in Table 2.

The reported weight percentages (wt%) were averaged between the collected spectra for each element. The remaining weight and atom percentages consisted of aluminum and oxygen consistent with the support material. A clear difference in the metal loading could be seen between the analyzed catalyst particles. The α-formulation made via sequential impregnation exhibited a significantly higher metal loading of both molybdenum and nickel. It has to be considered that this analysis is based on a single catalyst particle and it is possible that the catalyst particles could be unevenly loaded with the active metal. The low loading of iridium makes accurate quantification difficult, and the overlap of the iridium-M transition (1.977 keV) and the molybdenum L_l transition (2.015 keV) further complicates the quantification. The presence of iridium with a low concentration could be confirmed using the Ir-L_α transition (9.174keV). The Mo/Ni ratio was found to be similar for both formulation methods of the catalysts.

Table 2: Elemental composition of the α- and β-IrNiMo particle, determined via EDX. Average of the measured spectra

	α-IrNiMo		β-IrNiMo	
Element	wt%	at%	wt%	at%
Mo	12.3	3.10	9.15	2.24
Ni	3.38	1.40	2.15	0.86
Ir	0.31	0.04	0.41	0.05
Mo/Ni ratio		2.25		2.62

Before analysis of the PtNiMo-sample carbon deposition was performed to improve the conductivity of the sample, to allow for high resolution imaging. This allowed for the capture of more high resolution images, however as can be seen in Figure 4a) there was still charging of the surface which prohibited any real morphological investigations.

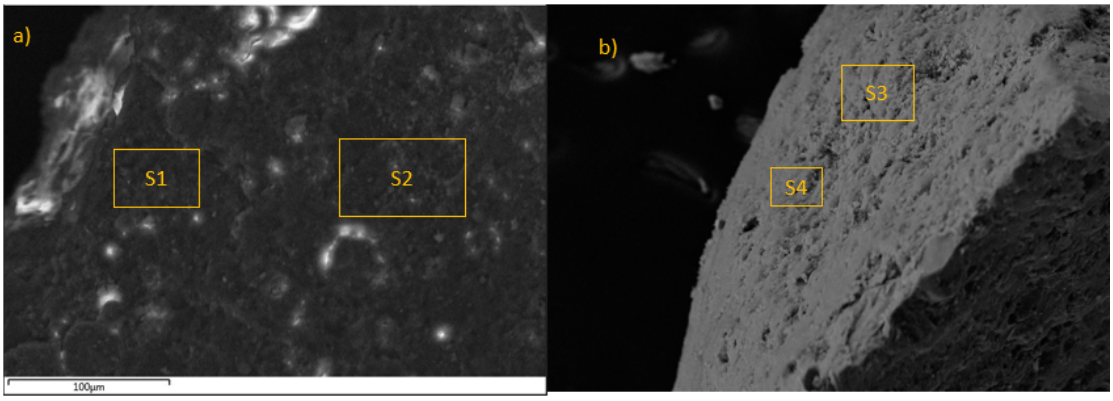

Figure 4: SEM micrographs with EDX collection areas highlighted, a) α-PtNiMo catalyst particle b) β-PtNiMo catalyst particle

The results from the quantification of the SEM-EDX spectra captured of the PtNiMo particles is shown in Table 3. A similar trend regarding the total molybdenum and nickel loading can be seen as with the IrNiMo catalysts. A higher loading was detected on the α-formulation, further suggesting that the difference in loading might be caused by the formulation method.

A higher loading than calculated during the synthesis of the catalyst was again measured on the α-formulation catalyst particle while the β-formulation exhibited a loading closer to the theoretical value. In contrast to the IrNiMo catalysts there is a large difference in the Mo/Ni ratio between the two formulations of the PtNiMo catalysts, with the β-formulation having a close to two times as high Mo/Ni ratio.

One theory explaining the high molybdenum loading of the measured catalysts is that the Mo which is impregnated first in all steps is enriched on the surface of the catalyst. To test this theory one of the α-particles were cut in half and a line-scan, where the electron beam is swept in a line over the catalyst particle, was performed from the edge to center of the particle along the cut surface. The results of which is shown in Figure 5.

Table 3: Elemental composition of the α- and β-PtNiMo particle, determined via EDX. Average of the measured spectra

	α-PtNiMo		β-PtNiMo	
Element	wt%	at%	wt%	at%
Mo	10.6	2.6	7.3	1.8
Ni	3.7	1.5	1.5	0.6
Pt	0.6	0.076	0.7	0.08
Mo/Ni ratio		1.73		2.98

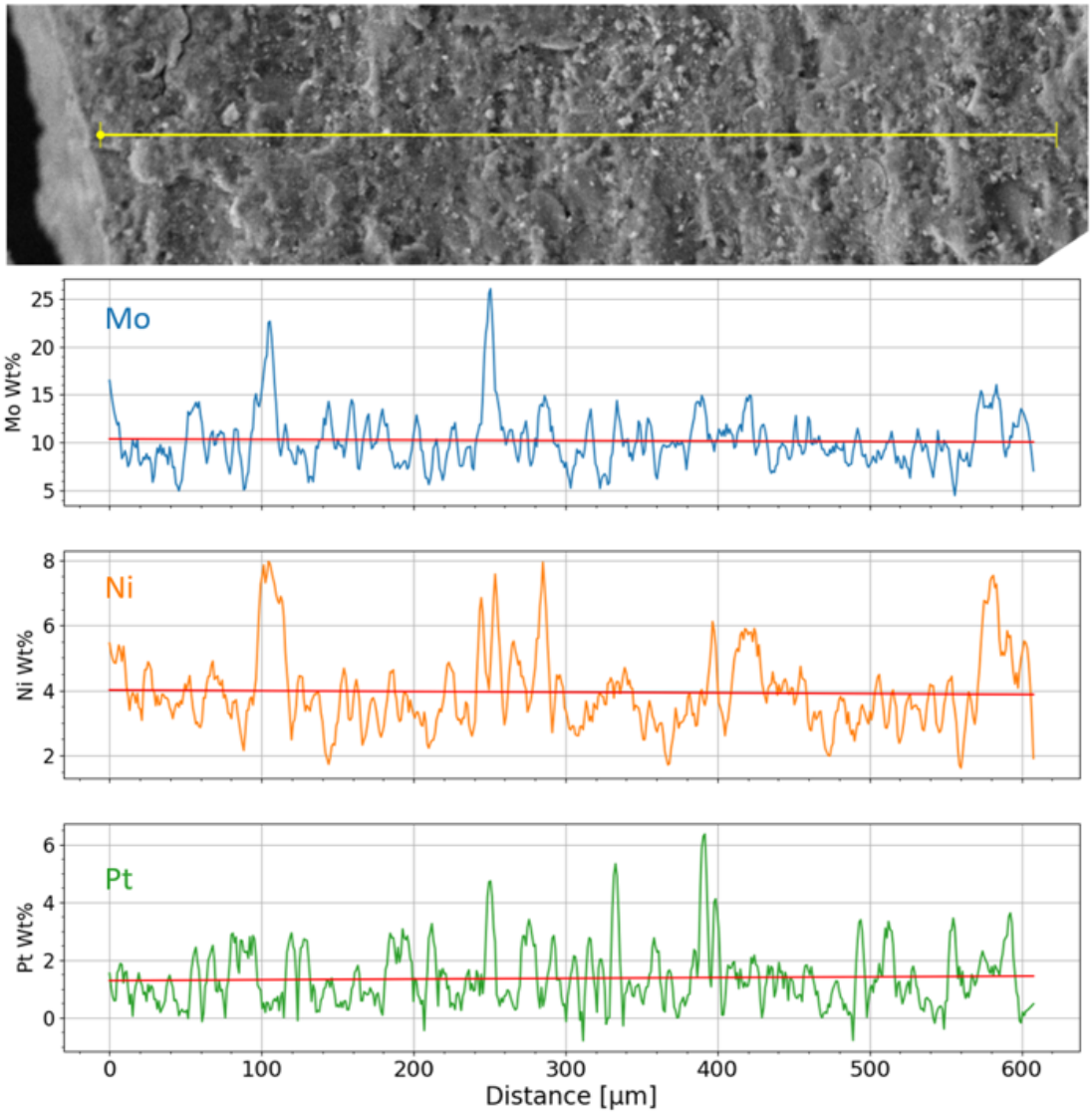

Figure 5: Line scan of a cut α-PtNiMo particle. The top image is a SEM micrograph over the scanned area. The red line in each component graph represent a linear fit to the composition over distance. Which indicates that there is no gradient in composition.

The line-scan over the cut surface did not indicate any trend of decreasing molybdenum content towards the center of the particle. The molybdenum content varied between 5 and 25wt% however the average molybdenum content was found to be approximately 10wt% which is consistent with the previous measurements reported in Table 3. This disproves the theory that the molybdenum is enriched on the surface of the particles.
The iridium and platinum variants both had the same trend of a higher molybdenum loading in the samples prepared with the α-method. In both cases the measured the loading was higher than the calculated theoretical loading during synthesis. Due to the fact that only one catalyst particle of each sample type was measured the high loading could be explained due to variations between the catalyst particles within each batch. The higher metal loading of the α-method can therefore be questioned and further SEM-EDX measurements are required to confirm this trend. A higher loading could mean that the α-impregnation method might be better at retaining the active metals and that would make it a superior method in that regard.

4.2 Reduction characteristics

4.2.1 Quantitative TPR

The calibration curve consisting of a series of TPR measurements with increasing mass of pure CuO powder, spanning from 10mg to 50mg, is shown in Figure 6. Due to the CuO powder being heavily influenced by static electricity no samples less than 10mg was able to be weighed with confidence in the results, and the precision of the weighing of the other CuO samples was reduced.

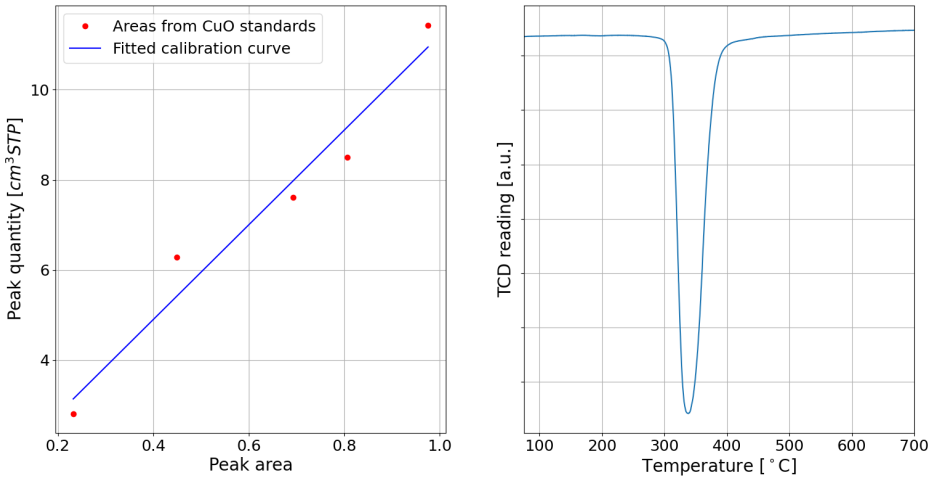

Figure 6: Left: Calibration curve relating the measured TPR peak area to the consumed amount of hydrogen. Right: Example CuO powder TPR curve, measured on 30mg of CuO powder.

This calibration curve was used to correlate peak areas in the TPR curves of the catalyst samples, with a corresponding hydrogen consumption.

4.2.2 Reference Ni, Mo and NiMo catalysts

To have a reference of the reduction behavior of the base components of the Ni-Mo catalyst systems a series of TPR measurements were performed on supported Ni, Mo and Ni-Mo catalysts, the results of which can be seen in Figure 7.

The results from the mono-metallic nickel catalysts show a main reduction peak, labeled c) in Figure 7, at 580°C. This main reduction peak is likely caused by the reduction of the NiO, the main form of nickel that is expected to be present on the oxidized catalyst. This reaction is shown in Reaction 2.

$$NiO + H_2 \xrightarrow{580\,^{\circ}C} Ni(\text{metal}) + H_2O \qquad \{2\}$$

Table 4: Areas of the primary and secondary reduction peaks of Mo/Al TPR curve Al_2O_3 [arbitrary units]

Area Peak b)	Area Peak e)
0.64 [a.u.]	1.22 [a.u]

The mono-metallic nickel TPR curve also displays a front and back shoulder of the to the main reduction peak at 400 and 800 °C respectively.

The origin of these shoulders or minor peaks is less obvious but a likely explanation often cited in literature is the presence of NiO structures with different support interactions or the formation of nickel-aluminum oxide structures. [24] The mono-metallic molybdenum catalyst displays two main reduction peaks, b) and e) at 440 and 880°C respectively.

Peak b) likely originates from the first reduction step of MoO_3 to MoO_2, which is shown in Reaction 2 Peak e) at the higher temperature of 880 °C, constitutes the second reduction stage to metallic molybdenum, which is described in reaction 3. The relative area, seen in table 4 between the first and second peak

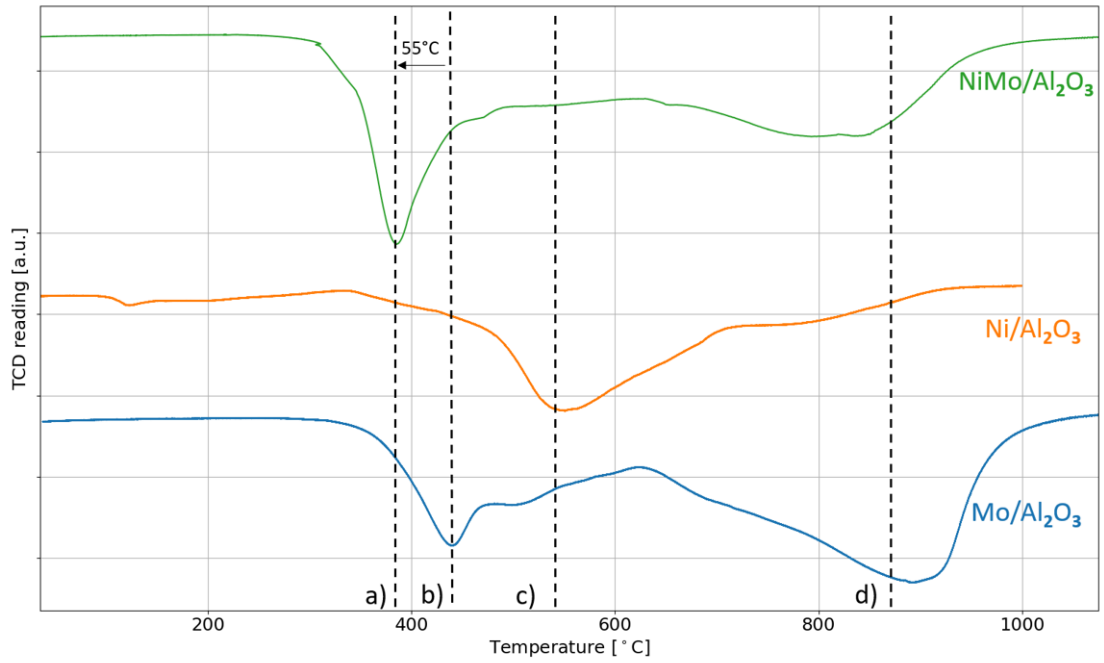

Figure 7: TPR curves for reference catalysts. The curves are offset vertically for clarity of viewing

is close to 1:2 which also supports the hypothesis that the two peaks arises from the sequential reduction of Reaction 3 followed by 4.

$$MoO_3 + H_2 \xrightarrow{440\,^\circ C} MoO_2 + H_2O \quad \{3\}$$

$$MoO_2 + 2\,H_2 \xrightarrow{880\,^\circ C} Mo(metal) + 2\,H_2O \quad \{4\}$$

This is also supported by results in literature. [31] The first molybdenum peak displays a shoulder which also likely is due to different surface structures of the MoO_3.

The TPR analysis of the $NiMo/Al_2O_3$ catalyst shows a similar reduction pattern as the mono-metallic Mo catalyst with two distinct peaks, peak a) and d). However, a shift in temperature of the first reduction peak to a reduction temperature 55°C lower than the $MoO_3 \longrightarrow MoO_2$ reduction peak. This shift in reduction temperature is indicative of the promoting effect the addition of nickel has to the catalyst system. The fact that the TPR curve produced from the $NiMo/Al_2O_3$ catalysts closely resembles the TPR curve for the Mo/Al_2O_3 catalyst suggests that the added nickel indeed has been incorporated into a single structure. In the case of two segregated structures of MoO_3 and NiO one would expect a second primary reduction peak corresponding to the reduction of $NiO \longrightarrow Ni(metal)$. A plateau/shoulder is present in the $NiMo/Al_2O_3$ curve at 550 °C, which could indicate a small presence of NiO. Further indications of the change of structure is given by the change of relative peak area between the primary and secondary reduction peak which can be seen in Table 5. One reaction sequence that could explain the results of the NiMo TPR curve is Reaction 5 followed by Reaction 6.

Table 5: Areas of the primary and secondary reduction peaks of $NiMo/Al_2O_3$ [arbitrary units]

Area Peak a)	Area Peak d)
0.75 [a.u.]	0.78 [a.u]

$$NiMoO_4 + 2\,H_2 \xrightarrow{385\,^\circ C} MoO_2 + Ni(metal) + 2\,H_2O \quad \{5\}$$

$$MoO_2 + 2\,H_2 \xrightarrow{800\,^\circ C} Mo(metal) + H_2O \quad \{6\}$$

The 1:1 ratio between the areas of peak a) and b), shown in Table 5, is indicative of that the amount of hydrogen consumed in both reactions should be the same. The total reduction of $NiMoO_4$ fits these criteria and this reduction sequence has been described in literature before. [13]

4.2.3 Iridium promoted catalysts

The synthesis of the α- and β-IrNiMo catalysts resulted in two batches of visually similar catalysts. The apparent homogeneity of the catalyst particles was high with most particles looking visually similar. However, a few alumina particles had a lighter coloring which could be an indicator of a different degree of coverage of the active metals. Due to the amount of sample used in each run of the TPR measurements these inhomogeneities are likely to have been average out. A similar observation could be observed for the other noble metal catalysts as well.

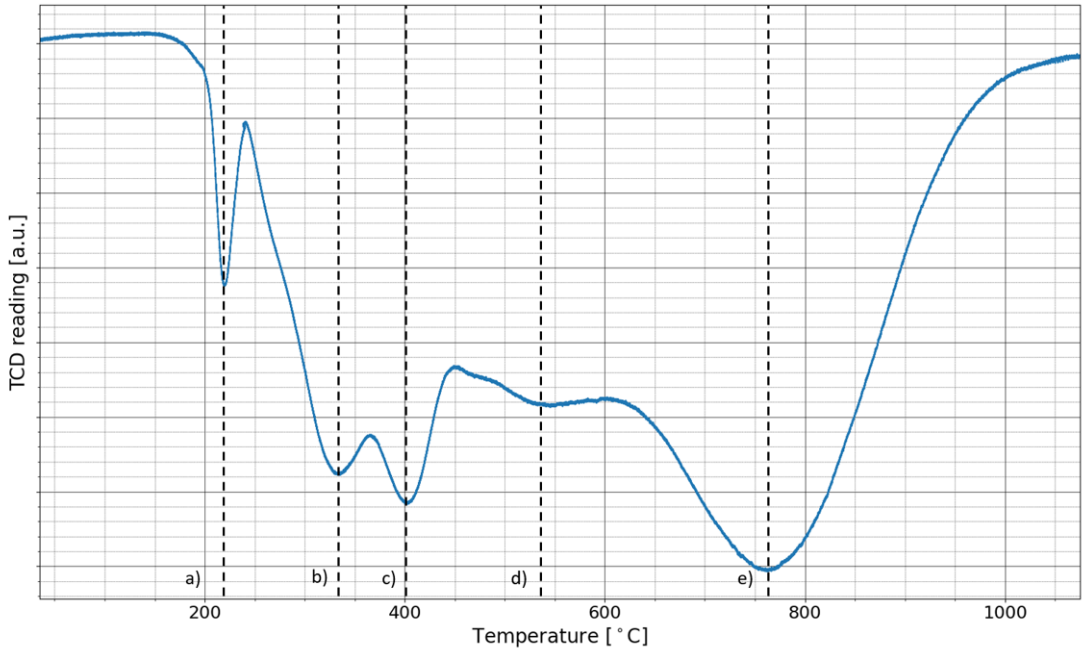

Figure 8: TPR profile of the α-IrNiMo/Al_2O_3 catalyst

The TPR measurements resulted in a more complex reduction profile, compared to the pure NiMo catalysts. A total of five reduction peaks could be identified in the profile, which can be seen in Figure 8. Comparing the reduction profile of the iridium promoted catalysts with the pure NiMo, additional peaks could be observed. The peak labeled a) in Figure 8 has a reduction temperature of 220°C which is significantly lower than any peak observed in the pure NiMo reduction curve.

The most likely explanation for the addition of this low temperature reduction peak is the reduction of some type of iridium oxide. By quantifying the corresponding hydrogen consumption of the reduction event captured in peak a), a more detailed analysis of the composition of the oxide can be made. The only documented iridium oxide is IrO_2, for which the total reduction reaction is shown in Reaction 7.

Table 6: Areas of the primary and secondary reduction peaks of NiMo/ Al_2O_3 [arbitrary units]

	Peak a)
Area [a.u.]	$2.4 \cdot 10^{-2}$
Calibrated H_2 consumption [mmol/g]	$4.7 \cdot 10^{-2}$
Equivalent Ir loading [wt%][1]	0.45%

$$IrO_2 + 2\,H_2 \longrightarrow Ir(\text{metal}) + 2\,H_2O \qquad \{7\}$$

[01] Based on case that the peak represents the total reduction of IrO_2

Based on the hypothesis that this peak is caused by the reduction of IrO_2, the iridium loading could be calculated. The loading was determined to be 0.45wt% which is very close to the theoretical 0.5% added in the synthesis of the catalyst. This would signify that iridium does not form any bi- or trimetallic oxides with nickel or molybdenum and is fully reduced in a separate event from any of the other metal oxides. Another relevant question is whether the result signifies that the IrO_2 is fully segregated from the $NiMoO_4$ on the surface of the catalyst support. Based on the TPR results this is a likely conclusion, but further studies are needed to confirm it. The addition of iridium also has a significant impact on the remaining reduction profile. What in the reduction profile of the un-promoted NiMo catalysts was a single reduction event at 390 °C, attributed to the reduction of $NiMoO_4$, has by the addition of iridium been separated into two peaks at 330°C and 400 °C respectively. The first of these peaks (b) has a significantly reduced reduction temperature, 55°C lower than peak a) in the pure NiMo curve, while the second (c) has a peak reduction temperature 10°C higher. One interpretation of these results is that reduction peak c) is attributed to the reduction of the same structures as in the original NiMo catalyst while peak b) has been structurally or environmentally influenced by the presence of iridium. Several polymorphs of $NiMoO_4$ has been characterized, and their bulk reducibility was studied by Rodriguez et al. [32] who found that the hydrated form of $NiMoO_4$ showed a higher reducibility and lower reduction temperature. One possible explanation of the lower reduction peak could be the formation of this type of $NiMoO_4$ polymorph, however this would have to be confirmed by further structural determination. There is also no apparent reason why the addition of iridium would allow for the formation of another polymorph, a different explantion may therefore be more likely. One such explanation could be related to the presence of iridium metal. Many noble metals are known to have a high affinity for hydrogen adsorption, it is possible that the presence of metallic iridium after the reduction of IrO_2 could catalyze the reduction of the surrounding $NiMoO_4$ by allowing for adsorption of hydrogen on the iridium metal. [33] For the presence of iridium metal to give rise to two separate reduction peaks the dispersion of the iridium would likely have to be poor, allowing for the coexistence of $NiMoO_4$ regions with and without iridium. The region of 500°C and above of the TPR profile does not show any large impact of the added iridium. A small peak/plateau at 550°C can be seen, this closely matches the reduction temperature of pure NiO which might indicate the presence of NiO on the sample.

The analysis of the co-impregnated IrNiMo samples, labeled β-IrNiMo together with a comparison between the sequentially impregnated sample, labeled α-IrNiMo can be seen in Figure 9. The low temperature region of all three samples show the reduction peak attributed to the reduction of IrO_2 at 220°C. The second reduction event, labeled peak b), occurs at a slightly lower temperature for the β-catalysts compared to the α-catalyst. Furthermore the second of the dual $NiMoO_4$ peaks, labeled c), previously found in the α-catalyst is not present in one of the β-sample TPR curves. There is a significant difference between the analysis results of the two β-samples, where sample -I has a more unstable TCD reading and exhibits a peak at approximately 380°C, which closely resembles peak c) in the α-IrNiMo profile. One possible explanation for these differences could be an uneven loading of iridium between catalyst particles, which could allow for catalyst particles to exhibit a different reduction behavior.

The differences between the α- and β-samples is interesting. Even though there are significant differences within measurements of the β-samples there is a tendency that more of the $NiMoO_4$ is reduced at a lower temperature for the β-variant. One explanation for this is that the iridium co-impregnated together with the nickel would have a more even distribution than the sequential impregnation. The better dispersion could allow for more of the $NiMoO_4$ to be influenced by the iridium, which could explain the disappearance of the second $NiMoO_4$ related reduction peak in one of the TPR curves.

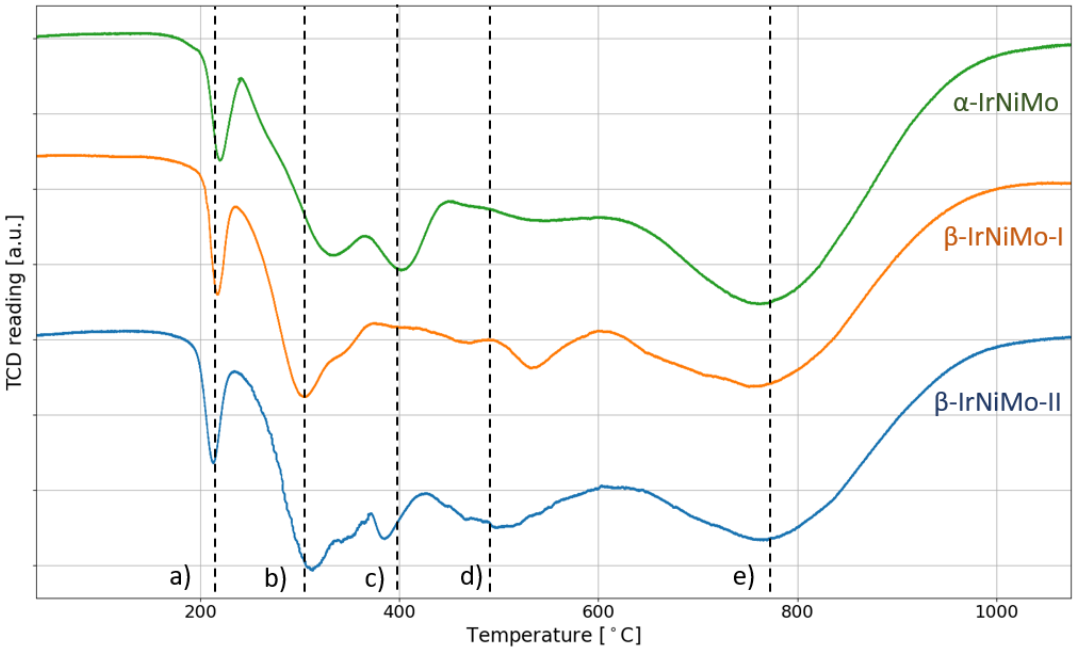

Figure 9: TPR profile for two co-impregnated IrNiMo/Al_2O_3 labeled β- compared with a sequentially impregnated sample labeled α-IrNiMo/Al_2O_3. The curves are offset vertically for readability

4.2.4 Platinum promoted catalysts

The results of the TPR measurements of both the α-PtNiMo and β-PtNiMo is shown in Figure 10, with two replicates of each shown as -I, and -II. Comparing these four TPR profiles with the previous Ir-promoted and pure NiMo measurements a clear change in the relative peak areas of in the low temperature range can be seen.

By quantifying the area of these low temperature reduction events, information about the total oxidation state of the compound being reduced could be deduced. The areas and the corresponding hydrogen consumption of peak a) is shown in Table 7.

Table 7: Areas of peak a) or a*) in Figure 10 [arbitrary units]

	α-PtNiMo-I	α-PtNiMo-II	β-PtNiMo-I	β-PtNiMo-II
Area [a.u.]	0.25	0.28	0.26	0.21
Calibrated H_2 consumption [mmol/g]	0.48	0.51	0.49	0.39

Based on the loading of the catalysts which was confirmed by the SEM-EDX quantification, a platinum oxide alone is unlikely to be responsible for the reduction peak. The amount of hydrogen consumed during this reduction event would correspond to a platinum oxide with a total oxidation state of +32 or with the formula PtO_{18}, which is not reasonable. It is therefore safe to assume that the addition of platinum induces reduction of nickel and molybdenum oxide at the low temperature of approximately 200°C a significant decrease in reduction temperature of 200°C. This would also explain the less pronounced peak b) at 400 °C where reduction of $NiMoO_4$ is thought to take place in the pure NiMo formulation. The fact that the reduction of the noble metal occurs simultaneously as the $NiMoO_4$ could suggest a different mechanism for this promoting effect than in the case of added iridium. One cause for this change in behaviour could be that platinum has been incorporated into the NiMo structure and therefore instantly

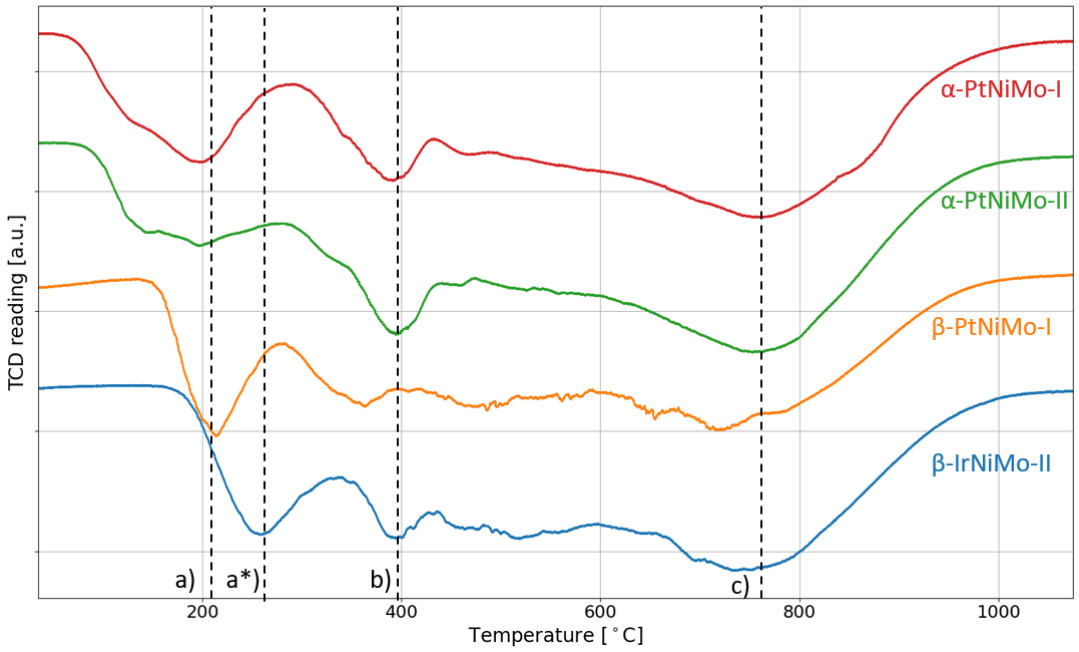

Figure 10: TPR of two sequentially impregnated PtNiMo samples, labeled α-PtNiMo/Al_2O_3 and two co-impregnated PtNiMo samples labeled β-PtNiMo/Al_2O_3. The curves are offset vertically for readability

causes the surround oxide to be reduced.

Comparing the two formulation methods for the PtNiMo samples does not show as a significant impact as for the IrNiMo. A similar trend with a less stable TCD signal in the temperature region of 400-600°C can be observed for the β- samples and the first reduction peak a) is more well defined for those samples as well. The sharper reduction peaks could signify a more homogeneous sample and that the NiMo oxide is more well dispersed.

4.2.5 Palladium promoted catalysts

An exploratory TPR experiment was performed on the α- PdNiMo catalysts, the results of which can be seen in Figure 11. The low temperature region of the TPR profile shows two large area peaks, something which was unexpected at the start of this study. This unexpected result was at the time explained by the ability of palladium to form metal hydrides, which would have made the TPR results challenging to interpret due to it being a secondary cause for hydrogen adsorption. Due to this hypothesis no more analyses were performed on the palladium samples, in favor of other samples.

After further analysis of the results, the conclusion that the dramatic change in the low temperature region of the TPR profile was caused by the formation of palladium hydride does not seem likely. Firstly, due to the low loading of palladium on the catalyst the amount of hydrogen able to dissolve would be very low. As shown in the results section 4.2.4 the Pt-promoted catalysts exhibit a similar effect in the low temperature region, without platinum being able to form such a hydride. There is an indication of there being two peaks in the low temperature area, which could correspond to a separate reduction of a palladium-oxide and the NiMo. However, there is a significant overlap between these peaks which make quantification or further identification difficult. What is clear is that the reduction of some type of NiMo structure occurs at a very low temperature with the initial peak occurring at 70°C and the start of a second at 100 °C. As with the previous catalysts there is a peak present at 400 °C, coinciding with the reduction temperature of un-promoted NiMo seen in Figure 7.

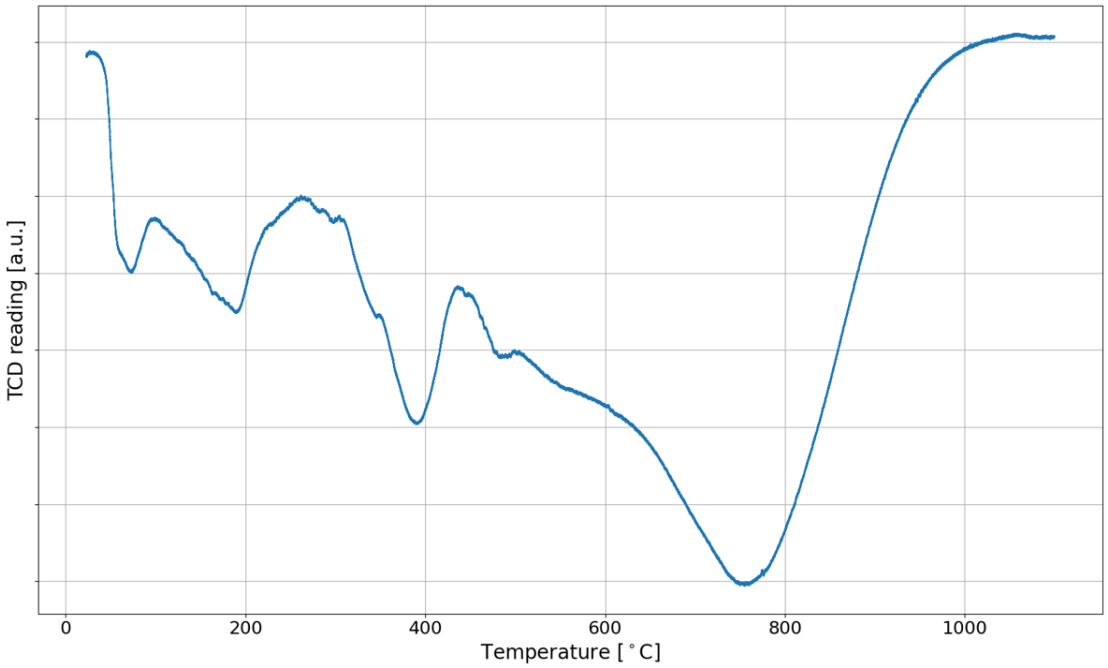

Figure 11: TPR profile of α-PdNiMo/Al_2O_3

5 Discussion

The addition of the three noble metals iridium, platinum and palladium all resulted in a clear change in the reduction temperature of the surrounding Ni-Mo oxide. The introduction of platinum and palladium lowered the onset of the reduction of $NiMoO_4$ with more than 200°C. Both the palladium and platinum promoted catalysts exhibited a reduction behavior where the reduction of the noble metal simultaneously induced reduction of the NiMo oxide. The possibility of this being caused by the formation of some palladium-nickel or platinum-molybdenum oxide is unlikely due to the large amount of hydrogen consumed in the TPR measurement. Due to the identical oxidation state of $NiMoO_4$ and the combined MoO_3 and NiO it is not possible to deduce whether or not the $NiMoO_4$ structure is intact and reduced in these early reduction events. In all promoted samples, except for one of the β-IrNiMo samples, a peak at approximately 400°C can be seen. This reduction temperature corresponds very well to the reduction peak assigned to $NiMoO_4$ of the non-promoted NiMo catalyst. One possible interpretation of this results is that not all of the $NiMoO_4$ is influenced by the presence of noble metals on the catalyst surface.
Continuing with the iridium-promoted catalysts, these exhibited a very different reduction profile than the other noble metals examined which could be an indication of a different promotion mechanism as described in Section 4.2.4. Gentry et Al. studied the promoting of noble metals on cupric oxides and suggested an effect called hydrogen spillover. [34] This effect is based on the ability of hydrogen to adsorb and dissociate on the surface of noble metals. These dissociated hydrogen atoms can then spillover onto the support, and subsequently impact the reduction of the surrounding oxide. This promotion mechanism could also be an explanation of the results observed in the iridium-TPR profiles. The primary reduction of iridium causes the formation metallic iridium islands which allows for adsorption of hydrogen that in turn can spillover to the NiMo oxide and causing an easier reduction. An illustration of the suggested promoting mechanism is shown in Figure 12. It is possible that the same mechanism could explain the TPR curves seen for platinum and palladium, but that the higher affinity for hydrogen allows for the immediate reduction of the surrounding oxide to occur.

A further possibility is that that palladium and platinum has the ability to be dissolved/be substituted into the $NiMoO_4$ structure which would allow for a direct and more intimate interaction with the surrounding structure. By having the noble metal directly integrated into the structure of the oxide it could also act as nucleation point for the reduction of the NiMo oxide lowering the energy barrier for the

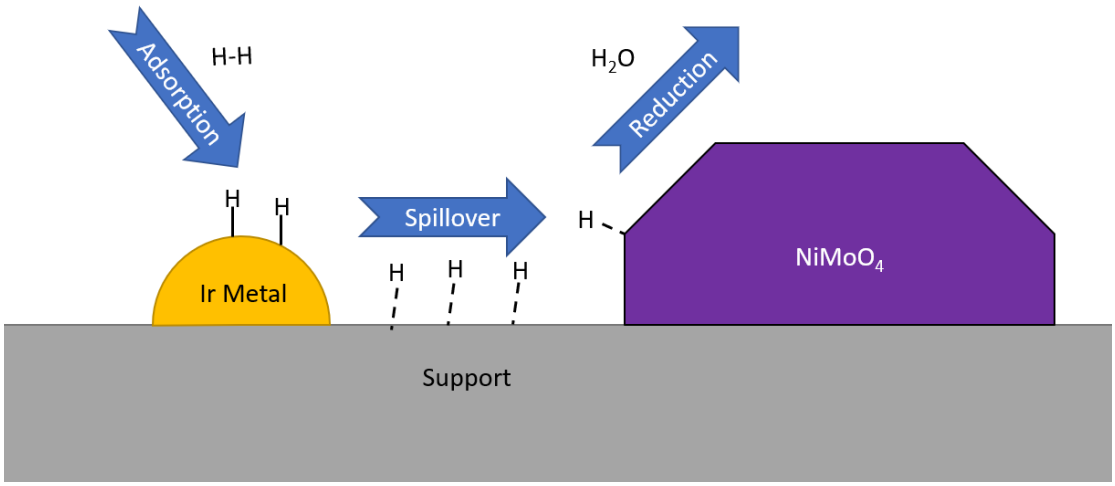

Figure 12: Hydrogen spillover, as the suggested promoting mechanism for iridium.

reduction.

A very important note when discussing the promotion ability of the noble metals is that further activity studies on model HDO compounds should be performed before any definite promotion ability in the HDO reaction is assigned to these compounds. Even though the enhanced reduction characteristics show promising results there are several questions which needs answering, such as; Is the $NiMoO_4$ structure intact with the addition of the noble metals? Is it still possible to form the important MoS_2 slab structures? And finally, and most important is there any improved catalytic activity? These questions should be answered before any final judgement about the promoting effects of NiMo-catalysts with noble metals in the HDO reaction can be done.

6 Conclusion

In this study Pt-, Ir- and Pd-NiMo/Al_2O_3 were synthesized using two different formulation methods and analyzed for their promoting ability. The chemical composition of the catalysts were analyzed using SEM-EDX and the promoting abilities were investigated by the reduction characteristics which was measured using TPR. The addition of the noble metals provided a clear improvement in the reducibility of the Ni-Mo catalysts studied, with a lowering of the reduction temperature with up to 200°C. Of the three studied noble metal promoters two different behaviors in the reduction of the surrounding oxide could be seen. Reduction of Ni-Mo catalysts promoted with platinum and palladium exhibited a simultaneous or very close to simultaneous reduction of the noble metal oxide together with the surrounding Ni-Mo oxide at a low temperature. While the iridium promoted catalysts exhibited a separation of approximately 100°C between the reduction of the noble metal and the remaining oxides. These different behaviors could be an indication of a different promotion mechanism. In the case of iridium, the separate reduction peaks could indicate that the promotion is a result of a secondary effect caused by the presence of iridium metal. One such secondary effect which could explain the changes seen in the reduction characteristics is hydrogen spillover from the reduced iridium to the NiMo oxide.

The two formulation methods studied showed limited differences for the platinum samples. For the iridium samples a shift to a lower reduction temperature could be seen for the β-formulation. The size of the reduction peak with a decreased reduction temperature was larger for the β-formulation, which could be interpreted as more of the sample being promoted. However, a large variability between experimental runs was found when analyzing the β-variants of iridium, which makes drawing conclusions more difficult. The improved reduction characteristics is a promising indication that shows that further studies into noble metal promoted NiMo catalysts is warranted.

7 Outlook and further investigations

This study has investigated the noble metal promoted catalysts strictly using characterization methods and even though the results are promising further studies of the catalysts is definitely needed before any conclusion about their HDO-activity can be made. Firstly, the natural next step in the evaluation of these catalysts is activity testing of the HDO reaction on model compounds. To gain further insight into the reduction mechanisms observed in this study *in-situ* X-ray Photoelectron Spectroscopy (XPS) and X-ray absorption fine structure (XAFS) would be able to provide structural and binding information about the active metals before, during and after the transitions seen. This could be used to verify that iridium indeed is reduced from its native oxide to its metallic form in the first reduction peaks observed at 200°C in figure 8. Furthermore, these methods could be used to investigate the oxidation state of platinum and palladium to figure out whether they are included in the NiMo-oxide structure or exists as separate nanoparticles. Another method that could be used to investigate the distribution of the different active metals is High Resolution Transmission Microscopy (HRTEM) or Scanning Transmission Electron Microscopy - Energy Dispersive X-ray spectroscopy (STEM-EDX). With these methods it could be possible to confirm the hypothesis that the iridium is dispersed as pure nanoparticle of IrO_2 by observing the distribution of the metals on the nanoscale.

References

[1] Abrar Inayat et al. “Techno-Economical Evaluation of Bio-Oil Production via Biomass Fast Pyrolysis Process: A Review”. In: *Frontiers in Energy Research* 9 (13, 2022). DOI: 10.3389/fenrg.2021.770355.

[2] Lu Qu et al. “A review of hydrodeoxygenation of bio-oil: model compounds, catalysts, and equipment”. In: *Green Chemistry* 23.23 (2021), pp. 9348–9376. DOI: 10.1039/D1GC03183J.

[3] P. M. Mortensen et al. “A review of catalytic upgrading of bio-oil to engine fuels”. In: *Applied Catalysis A: General* 407.1 (4, 2011), pp. 1–19. DOI: 10.1016/J.APCATA.2011.08.046.

[4] Tatiana Klimova, Paola Mendoza Vara, and Ivan Puente Lee. “Development of new NiMo/γ-alumina catalysts doped with noble metals for deep HDS”. In: *Catalysis Today* 150.3 (30, 2010), pp. 171–178. DOI: 10.1016/J.CATTOD.2009.08.003.

[5] Soosan Kim et al. “Recent advances in hydrodeoxygenation of biomass-derived oxygenates over heterogeneous catalysts”. In: *Green Chemistry* 21.14 (15, 2019), pp. 3715–3743. DOI: 10.1039/C9GC01210A.

[6] Houman Ojagh. “Hydrodeoxygenation (HDO) catalysts Characterization, reaction and deactivation studies”. PhD thesis. Chalmers University Of Technology, 2018.

[7] J. A. Cecilia et al. “Enhanced HDO activity of Ni_2P promoted with noble metals”. In: *Catalysis Science & Technology* 6.19 (2016), pp. 7323–7333. DOI: 10.1039/C6CY00639F.

[8] Joseph Shabtai et al. “Catalytic functionalities of supported sulfides: V. CN bond hydrogenolysis selectivity as a function of promoter type”. In: *Journal of Catalysis* 113.1 (1, 1988), pp. 206–219. DOI: 10.1016/0021-9517(88)90249-7.

[9] A. Jos van Dillen et al. “Synthesis of supported catalysts by impregnation and drying using aqueous chelated metal complexes”. In: *Journal of Catalysis* 216.1 (1, 2003), pp. 257–264. DOI: 10.1016/S0021-9517(02)00130-6.

[10] Quan Shi and Jianxun Wu. “Review on Sulfur Compounds in Petroleum and Its Products: State-of-the-Art and Perspectives”. In: *Energy & Fuels* 35.18 (16, 2021), pp. 14445–14461. DOI: 10.1021/acs.energyfuels.1c02229.

[11] M. Daage and R. R. Chianelli. “Structure-Function Relations in Molybdenum Sulfide Catalysts: The ”Rim-Edge” Model”. In: *Journal of Catalysis* 149.2 (1, 1994), pp. 414–427. DOI: 10.1006/JCAT.1994.1308.

[12] Joaquın L. Brito and A. Liliana Barbosa. “Effect of Phase Composition of the Oxidic Precursor on the HDS Activity of the Sulfided Molybdates of Fe(II), Co(II), and Ni(II)”. In: *Journal of Catalysis* 171.2 (15, 1997), pp. 467–475. DOI: 10.1006/jcat.1997.1796.

[13] Joaqun L. Brito, Jorge Laine, and Kerry C. Pratt. “Temperature-programmed reduction of Ni-Mo oxides”. In: *Journal of Materials Science* 24.2 (1989), pp. 425–431. DOI: 10.1007/BF01107422.

[14] P. Arnoldy et al. “Temperature-programmed sulfiding of MoO3Al2O3 catalysts”. In: *Journal of Catalysis* 92.1 (1, 1985), pp. 35–55. DOI: 10.1016/0021-9517(85)90235-0.

[15] R. R Chianelli et al. “Periodic trends in hydrodesulfurization: in support of the Sabatier principle”. In: *Applied Catalysis A: General* 227.1 (8, 2002), pp. 83–96. DOI: 10.1016/S0926-860X(01)00924-3.

[16] Wei Jin et al. “Noble Metal Supported on Activated Carbon for “Hydrogen Free” HDO Reactions: Exploring Economically Advantageous Routes for Biomass Valorisation”. In: *ChemCatChem* 11.17 (2019), pp. 4434–4441. DOI: 10.1002/cctc.201900841.

[17] Dhrubojyoti D. Laskar et al. “Noble-metal catalyzed hydrodeoxygenation of biomass-derived lignin to aromatic hydrocarbons”. In: *Green Chemistry* 16.2 (28, 2014), pp. 897–910. DOI: 10.1039/C3GC42041H.

[18] Zdeněk Vıt, Josef Cinibulk, and Daniela Gulková. “Promotion of Mo/Al2O3 sulfide catalyst by noble metals in simultaneous hydrodesulfurization of thiophene and hydrodenitrogenation of pyridine: a comparative study”. In: *Applied Catalysis A: General* 272.1 (28, 2004), pp. 99–107. DOI: 10.1016/j.apcata.2004.05.037.

[19] Mohammad M. Hossain. “Influence of noble metals (Rh, Pd, Pt) on Co-saponite catalysts for HDS and HC of heavy oil”. In: *Chemical Engineering Journal* 123.1 (1, 2006), pp. 15–23. DOI: 10.1016/j.cej.2006.07.003.

[20] P.A. Webb, C. Orr, and Micromeritics Instrument Corporation. *Analytical Methods in Fine Particle Technology*. Micromeritics Instrument Corporation, 1997.

[21] Alan Jones. *Tempature-programmed reduction for solid materials characterization*. Vol. 24. CRC Press, 1986. DOI: https://doi.org/10.1201/9781498710497.

[22] Daniele A.M. Monti and Alfons Baiker. “Temperature-programmed reduction. Parametric sensitivity and estimation of kinetic parameters”. In: *Journal of Catalysis* 83.2 (1, 1983), pp. 323–335. DOI: 10.1016/0021-9517(83)90058-1.

[23] Isabela Alves de Castro et al. “Molybdenum Oxides – From Fundamentals to Functionality”. In: *Advanced Materials* 29.40 (2017), p. 1701619. DOI: 10.1002/adma.201701619.

[24] Chiuping Li and Yu-Wen Chen. “Temperature-programmed-reduction studies of nickel oxide/alumina catalysts: effects of the preparation method”. In: *Thermochimica Acta* 256.2 (1, 1995), pp. 457–465. DOI: 10.1016/0040-6031(94)02177-P.

[25] Jonas Elmroth Nordlander. “Nanoscale characterisation of model Ni-Mo catalyst active phases”. Lund University, 2022.

[26] Hansaem Jang and Jaeyoung Lee. “Iridium oxide fabrication and application: A review”. In: *Journal of Energy Chemistry* 46 (1, 2020), pp. 152–172. DOI: 10.1016/j.jechem.2019.10.026.

[27] Chin-Pei Hwang and Chuin-Tih Yeh. “Platinum-oxide species formed by oxidation of platinum crystallites supported on alumina”. In: *Journal of Molecular Catalysis A: Chemical* 112.2 (25, 1996), pp. 295–302. DOI: 10.1016/1381-1169(96)00127-6.

[28] Z A Munir and P G Coombs. “The oxidation-reduction kinetics of palladium powder”. In: *Metallurgical Transactions B* 14 (1983), pp. 95–99.

[29] Debbie J Stokes. “Principles of SEM”. In: *Principles and Practice of Variable Pressure/Environmental Scanning Electron Microscopy (VP-ESEM)*. 2008. Chap. 2, pp. 17–62. DOI: https://doi.org/10.1002/9780470758731.ch2.

[30] Sara Blomberg et al. “Bimetallic Nanoparticles as a Model System for an Industrial NiMo Catalyst”. In: *Materials* 12.22 (2019), p. 3727. DOI: 10.3390/ma12223727.

[31] John R. Regalbuto and Jin -Wook Ha. “A corrected procedure and consistent interpretation for temperature programmed reduction of supported MoO3”. In: *Catalysis Letters* 29.1 (1994), pp. 189–207. DOI: 10.1007/BF00814265.

[32] José A. Rodriguez et al. “Reaction of H_2 and H_2S with $CoMoO_4$ and $NiMoO_4$: TPR, XANES, Time-Resolved XRD, and Molecular-Orbital Studies”. In: *The Journal of Physical Chemistry B* 103.5 (1, 1999), pp. 770–781. DOI: 10.1021/jp983115m.

[33] Changqing Li and Jong-Beom Baek. “Recent Advances in Noble Metal (Pt, Ru, and Ir)-Based Electrocatalysts for Efficient Hydrogen Evolution Reaction”. In: *ACS Omega* 5.1 (18, 2019), pp. 31–40. DOI: 10.1021/acsomega.9b03550.

[34] Stephen J. Gentry, Nicholas W. Hurst, and Alan Jones. “Study of the promoting influence of transition metals on the reduction of cupric oxide by temperature programmed reduction”. In: *Journal of the Chemical Society, Faraday Transactions 1: Physical Chemistry in Condensed Phases* 77.3 (1981), p. 603. DOI: 10.1039/f19817700603.